NF-κB Induction by Bisperoxovanadium Compounds Requires CD45, p36^{LAT}, PKC, and IKK Activity and Exhibits Kinetics of Activation Comparable to Those of TCR/CD28 Coengagement†

Michel Ouellet,‡ Jocelyn Roy,‡ Benoit Barbeau,‡ Romas Geleziunas,§ and Michel J. Tremblay*,‡

Centre de Recherche en Infectiologie, Hôpital CHUL, Centre Hospitalier Universitaire de Québec, and Département de Biologie Médicale, Faculté de Médecine, Université Laval, Ste-Foy, Québec, Canada G1V 4G2, and Merck Research Laboratories, West Point, Pennsylvania 19486

Received January 7, 2003; Revised Manuscript Received April 17, 2003

ABSTRACT: We have previously shown that bisperoxovanadium (bpV) phosphotyrosyl phosphatase inhibitors can potently activate NF-κB. We have already determined that p56^{lck}, ZAP-70, SLP-76, capacitative entry of calcium, and calcium-regulated effectors are important in bpV-induced NF-κB activation. In this study, we evaluated whether other signal transducers previously reported in NF-κB induction by T cell activating stimuli are also activated by bpV compounds. Nuclear translocation of NF-κB was evaluated in cell lines deficient for either CD45 or p36^{LAT} to assess the role of these signal transducers in bpV-mediated NF-κB activation. A deficiency of either protein greatly reduced the extent of NF-κB nuclear translocation following bpV treatment. Isoform-specific PKC inhibitors were then used to show that bpV compounds activate NF-κB through both calcium-sensitive and -insensitive PKC isoforms. The implication of the IκB−kinase complex was then investigated through the use of an IκBα-specific kinase assay and plasmids expressing catalytically inactive forms of IKKα and IKK*β*. Upstream kinases involved in IKK complex activation such as TPL-2/COT, NIK, and IKKε were also shown to play an important role in bpV-mediated NF-κB activation. Finally, reporter gene transcriptional assays and gel shift assays were performed to compare the kinetics of activation of NF-κB by bpV with those of antigenic and TNFα stimulation. We demonstrate, both in Jurkat cells and in primary T cells, that bpV-mediated NF-κB activation kinetics are comparable to those of an antigenic stimulation but occur much slower than the kinetics seen upon TNFα treatment.

The elaboration of a specific immune response necessitates the precise control of cellular activation and a highly regulated intracellular environment for mounting a specific response against a microbial pathogen. One key player in the development of a strong immune response following T cell activation is the NF-κB transcription factor that is responsible for potent induction of many cytokines and adhesion molecules.

NF-κB is a hetero- or homodimeric transcription factor composed of members of the Rel family that includes RelA (p65), RelB, c-rel, p50, and p52, the most studied of which remain p50 and RelA. In its inactive state, NF-κB is retained in the cytoplasm by its natural inhibitors, the IκBs (*1*). Five members of this family are known to exist (IκBα, IκB*β*, IκB*γ*, IκBε, and Bcl-3), of which IκBα is by far the most intensively studied. Following cellular activation via either antigenic stimulation or proinflammatory cytokines such as TNFα and IL-1, IκBα is phosphorylated on two critical serines (*2*) which triggers ubiquitination of two adjacent lysines (*3*). Ubiquitination tags IκBα for degradation by the 26S proteasome with the final result that NF-κB enters the nucleus through unmasking of a nuclear localization signal (*4*). Translocation of free NF-κB to the nucleus allows it to bind to specific DNA sequences and amplify the transcription of multiple genes implicated in immunity and protection from apoptosis.

One of the first events following T cell receptor (TCR) engagement by a complex made of a peptide and a major histocompatibility complex (MHC) molecule is the tyrosine phosphorylation of the ζ chain of the CD3 complex by the *src* family protein tyrosine kinase p56^{lck} (*5*). This primordial event initiates the recruitment and activation of the *syk* family PTK[1] ZAP-70 (*6*−*8*), which leads to the formation of an activated complex capable of phosphorylating p36^{LAT} (*9*, *10*). This in turn allows the recruitment of multiple signaling molecules, including Tec family kinases (*11*−*15*), Vav (*16*), Nck (*17*), SLP-76, and the RhoA family of small guanine nucleoside triphosphatase (GTPase) (*17*), phosphatidylinositol 3-kinase (PI3K), Ras, and phospholipase C*γ* (PLC*γ*) (*10*). These effectors make up the starting point of a highly ordered and specific signaling amplification pathway that will ultimately lead to cellular proliferation, differentiation, or apoptosis. Because all of these processes stem from the initial

† M.O. is the recipient of a CIHR doctoral research award, and M.J.T. holds a Tier 1 Canada Research Chair in Human Immuno-Retrovirology. This work was supported in part by Grant HOP-15575 to M.J.T. from the Canadian Institutes of Health Research (CIHR) HIV/AIDS Program.

* To whom correspondence should be addressed: Laboratoire d'Immuno-Rétrovirologie Humaine, Centre de Recherche en Infectiologie, RC709, Hôpital CHUL, Centre Hospitalier Universitaire de Québec, 2705 boul. Laurier, Ste-Foy, Québec, Canada G1V 4G2. Phone: (418) 654-2705. Fax: (418) 654-2212. E-mail: Michel.J.Tremblay@crchul.ulaval.ca.

‡ Centre Hospitalier Universitaire de Québec and Université Laval.

§ Merck Research Laboratories.

10.1021/bi034013b CCC: $25.00
Published on Web 06/19/2003

tyrosine phosphorylation of the CD3 ζ chain, this event is under tight regulation. Two antagonizing classes of enzymes, namely, the protein tyrosine kinases (PTKs) and the protein tyrosine phosphatases (PTPs), assume the vital role of maintaining optimal levels of tyrosine-phosphorylated substrates. Increased levels of tyrosine phosphorylation can thus occur following either an upregulation of PTK activity or a downregulation of PTP activity, which is the premise behind the use of PTP inhibitors as cellular activators. Many groups have reported cellular activation following treatment of T cells with pervanadate, a very well-known PTP inhibitor that is composed of a mixture of sodium orthovanadate and hydrogen peroxide (*18*−*21*). In this reaction, sodium orthovanadate becomes oxidized and is thus highly reactive against sulfhydryl groups. The structure of pervanadate is highly similar to a transition state of a phosphate group during the dephosphorylation reaction which allows it to easily enter the catalytic site of the PTP. Once inside the catalytic cleft, it can oxidize a critical cysteine residue located at the bottom of the active site, thereby irreversibly inhibiting the enzyme (*22*).

Pervanadate is composed of many different molecules with different oxidation states and is therefore an unstable heterogeneous mixture. Consequently, to increase the stability of these compounds, an ancillary ligand has been added to the outer coordination sphere of the vanadium core. Attempts to purify one specific type of molecule using ^{51}V nuclear magnetic resonance gave rise to the bisperoxovanadium (bpV) compounds (*23*). These compounds are 95% pure and contain two oxo groups and one oxyanion group. Moreover, functional studies using different bpV compounds revealed that ancillary ligands conferred an increased specificity on such molecules (*23*).

In this report, we further elucidated the NF-κB signaling cascade activated by bpV compounds and found striking similarities with the signaling pathways initiated by the physiological TCR/CD28 costimulation. In addition to previously discovered intracellular second messengers (*24*), we demonstrate the critical role of the protein tyrosine phosphatase CD45 and the molecular adapter $p36^{LAT}$, as well as the implication of multiple kinases of the IKK family and regulators of IKKs such as PKC in the signaling cascade initiated by bpV compounds. Moreover, kinetic experiments with NF-κB-mediated transcriptional activation and NF-κB nuclear translocation show a better correlation between TCR/CD28- and bpV-derived signals compared to those induced by the proinflammatory cytokine TNFα in both immortalized and primary human CD4-positive T lymphocytes.

EXPERIMENTAL PROCEDURES

Cell Lines. The lymphoid T cell lines used in this study include Jurkat (clone E6.1) and JCAM.2 cells. The Jurkat line is considered a model cell line for the study of T cell signaling machinery (*25*), while the JCAM.2 line is a derivative of the Jurkat leukemic T cell line which is deficient in $p36^{LAT}$ expression (*9*, *26*). Likewise, the J45.01 line is a Jurkat-derived cell line deficient in CD45 expression (*27*). DT30 cells are stably transfected with a human B7.1 expression vector and were derived from the P815 mastocytoma cell line which expresses the FcγRI receptor (American Type Culture Collection, Manassas, VA). The Jurkat-derived NF-κB reporter cell line JκB stably expresses the firefly luciferase gene under the control of five consensus NF-κB binding sites (*24*). All cell lines were grown in RPMI medium containing 10% fetal calf serum (Invitrogen Corp., Carlsbad, CA), L-glutamine (2.92 μg/mL; Invitrogen Corp.), penicillin G (1 unit/mL; Invitrogen Corp.), and streptomycin sulfate (1 μg/mL; Invitrogen Corp.). When necessary, G418 (Invitrogen Corp.) was added to the cell culture medium at a concentration of 1 mg/mL. Peripheral blood mononuclear cells (PBMCs) were obtained from healthy donors and purified by Ficoll-Paque centrifugation. PBMCs were maintained in RPMI medium (described above) containing 1 μg/mL PHA-L and 50 units/mL of IL-2 for 1 week. CD4+ T lymphocytes were derived from these cultures through the use of a negative purification kit involving StemSep magnetic beads (StemCell Technologies, Vancouver, BC). Briefly, we have used an antibody cocktail and a magnetic colloid that deplete the cell population of every cell type except CD4+ T lymphocytes upon application to a magnetically charged column. Prior to stimulation, total PBMCs or purified CD4-expressing T lymphocytes were starved in IL-2 for 1 day to enable them to return to a resting state.

Plasmids. The expression vector for $p36^{LAT}$, pCDNA3.1 LAT, was generously provided by A. Weiss (University of California, San Francisco, CA) (*9*). The expression vector encoding the luciferase gene under the control of five consensus binding sites for NF-κB (pNF-κB-LUC) was purchased from Stratagene (La Jolla, CA). Vectors encoding enzymatically inactive IKKα and IKKβ (pEV3T T7 IKKα K44M and pCDNA3.1 IKKβ K44A) as well catalytically inactive versions of NIK and TPL-2/COT [pRK5myc TPL-2/COT K167M and pRKmyc NIK KK(429/430)AA] were described previously (*27*, *28*). The dominant negative IKKε expression vector (pCDNA3.1 IKKε K38A) was obtained from T. Maniatis (Harvard University, Cambridge, MA) and was previously described (*29*).

Electroporation. Cells were electroporated using a gene pulser I apparatus (Bio-Rad, Hercules, CA) (960 μF, 250 V) at room temperature. Cells were first concentrated at a density of 37.5×10^6 cells/mL in RPMI medium (described above) and then electroporated either with 5 μg of reporter construct DNA alone or, in the case of $p36^{LAT}$ reconstitution experiments, with 5 μg of reporter construct DNA and 0, 10, or 20 μg of pCDNA3.1 LAT wt plasmid. The total DNA amount for the reconstitution experiments was kept constant at 25 μg using the control plasmid pCDNA3.1.

Cell Stimulation. Cells (1×10^5 per well) were seeded on a 96-well plate and, depending on the experiments, were stimulated with PMA (Sigma, St. Louis, MO) at 20 ng/mL, PHA-P (Sigma) at 3 μg/mL, ionomycin (Sigma) at 1 μM, or TNFα (R&D Systems, Minneapolis, MN) at 20 ng/mL. The bpV compound harboring as an ancillary ligand pyridine-2-carboxylic acid anion (bpV[pic]; Alexis Corp., San Diego,

[1] Abbreviations: bpV[pic], bisperoxovanadium pyridine-2-carboxylic acid anion; LAT, linker for activation of T cells; PI3-K, phosphatidylinositol 3-kinase; PLC, phospholipase C; SLP-76, 76 kDa SH2 domain-containing leukocyte protein; ZAP-70, 70 kDa ζ chain-associated protein; IKK, IκB kinase; NIK, NF-κB inducing kinase; NEMO, NF-κB enhancer and modulator; MAP, mitogen-activated protein; MAPK, MAP kinase; ERK, extracellularly regulated kinase; MEK, MAPK/ERK kinase; MEKK, MEK kinase; PKC, protein kinase C; PTK, protein tyrosine kinase; PTP, protein tyrosine phosphatase; PFA, paraformaldehyde; SDS, sodium dodecyl sulfate.

CA) was always added at a subcytotoxic and subcytostatic concentration of 10 μM. For DT30 or P815 cells, OKT3 was used at a concentration of 40 μg/mL with paraformaldehyde (PFA)-fixed cells (2×10^6/mL). Fixed OKT3-bearing DT30 or P815 cells were used to stimulate Jurkat cells at a ratio of one DT30 or P815 cell per 10 Jurkat cells (yields 2 μg/mL OKT3). For the PKC inhibition experiments, the calcium-sensitive PKCα and PKCβ inhibitor Gö6976 and the calcium-insensitive PKCθ and PKCδ inhibitor Rottlerin were both purchased from Calbiochem (La Jolla, CA).

IκB Kinase Assay. Following stimulation, Jurkat cells (1×10^7) were centrifuged and resuspended in 500 μL of lysis buffer [50 mM HEPES (pH 7.4), 250 mM NaCl, 1% (v/v) NP-40, 1 mM EDTA, 1 mM PMSF, 5 mM NaF, 20 μg/mL aprotinin, and 20 μg/mL leupeptin]. Endogenous IKKs were immunoprecipitated using an IKKα/IKKβ cross-reactive antibody (anti-IKKα/H744, Santa Cruz Biotechnology, Santa Cruz, CA) and A/G plus agarose beads (Santa Cruz Biotechnology). After extensive washes, immunoprecipitates were finally resuspended in 20 μL of kinase reaction mix [10 mM HEPES (pH 7.4), 1 mM $MnCl_2$, 5 mM $MgCl_2$, 12.5 mM glycerol 2-phosphate, 50 μM Na_3VO_4, 2 mM NaF, 500 μM DTT, and 10 μM ATP] added along with 1 μg of purified IκBα (1−317) (Santa Cruz Biotechnology) and 5 μCi of [γ-^{32}P]ATP (Perkin-Elmer, Boston, MA) and incubated for 1 h at 30 °C. SDS loading buffer was added to the kinase reaction products which were then boiled for 5 min and frozen until SDS−PAGE and transfer were performed. Kinase reaction products were loaded on a 10% SDS−PAGE gel and run for 2 h at 130 V. The polyacrylamide gel was then electrotransferred on a PVDF membrane which was autoradiographed overnight at −85 °C on Kodak BioMax MR film. The membrane was then probed with an IκBα-specific antibody (Santa Cruz Biotechnology) to evaluate the loading quality of kinase products.

Luciferase Assay. Luciferase activity was monitored using a previously described protocol (*30*). Briefly, 100 μL of cell-free supernatant was removed from each well of a 96-well plate, and 25 μL of 5× lysis buffer [25 mM Tris-phosphate (pH 7.8), 2 mM dithiothreitol, 1% Triton X-100, and 10% glycerol] was added. After vigorous agitation for 30 min and one cycle of freezing and thawing, 20 μL of cellular extract was transferred to a 96-well luminometer plate, and luciferase activity was monitored on a Dynex MLX microplate luminometer for 20 s/well after a 2 s delay following addition of 100 μL of luciferase buffer [20 mM Tricine, 1.07 mM $(MgCO_3)_4 \cdot Mg(OH)_2 \cdot 5H_2O$, 2.67 mM $MgSO_4$, 0.1 mM EDTA, 220 μM coenzyme A, 4.70 μM D-Luciferin potassium salt, 530 μM ATP, and 33.3 mM dithiothreitol].

Nuclear Extract Preparations. Nuclear extracts were prepared according to a previously described protocol (*30*). Briefly, unstimulated or activated cells (5×10^6) were first washed with cold phosphate-buffered saline (PBS). Cells were then resuspended in 400 μL of hypotonic buffer [10 mM HEPES (pH 7.9), 10 mM KCl, 0.1 mM EDTA, 0.1 mM EGTA, 1 mM DTT, and 0.5 mM PMSF] and kept on ice for 15 min before lysis with 25 μL of 10% NP-40. After a brief vortexing and centrifugation, the supernatant was discarded and the nuclei-containing pellet was resuspended in hypertonic buffer [20 mM HEPES (pH 7.9), 0.4 M NaCl, 1 mM EDTA, 1 mM EGTA, 1 mM DTT, and 1 mM PMSF] followed by gentle agitation for 15 min. The solution was then centrifuged, and the protein concentration was measured in the supernatant by the BCA assay (Pierce, Rockford, IL) before storage at −85 °C until use.

Probe Labeling. Radioactive labeling of an oligonucleotide containing a NF-κB binding site (5′-ATGTGAGGGGACTTTCCCAGGC-3′) was performed by adding 50 ng of one of the DNA strands in a T4 polynucleotide kinase buffer containing 30 μCi of [γ-^{32}P]ATP and T4 polynucleotide kinase and incubating the mixture for 30 min at 37 °C. The reaction was stopped by the addition of 5 μL of 0.2 M EDTA and 25 μL of H_2O. A phenol/chloroform extraction of the oligonucleotide was then performed, after which the aqueous phase was spun through a G50 Sephadex column for further purification. The oligonucleotide was then allowed to hybridize overnight with 200 ng of the complementary strand in an annealing buffer [100 mM NaCl, 5 mM Tris (pH 7.5), 10 mM $MgCl_2$, 20 μM EDTA, and 1 mM DTT] after being heated at 90 °C for 2 min.

Electrophoretic Mobility Shift Assay (EMSA). Nuclear extracts (10 μg) were mixed with poly(dI-dC) (1 μg/mL), bovine serum albumin (1 μg/mL), and the labeled oligonucleotide in binding buffer [100 mM HEPES (pH 7.9), 40% glycerol, 10% Ficoll, 250 mM KCl, 10 mM dithiothreitol, 5 mM EDTA, and 250 mM NaCl]. This mixture was incubated for 20 min at room temperature and then run through a 4% (w/v) polyacrylamide gel for 2 h at 150 V. Competition experiments were performed with a 100-fold excess of cold oligonucleotides harboring NF-κB (specific competition) or AP-1 binding sequences (5′-CGCTTGATGACTCAGCCGGAA-3′) which served as a nonspecific competitor. Gels were dried and exposed to Kodak Biomax MR film at −85 °C.

Cytofluorometry. Total PBMCs and purified CD4+ T lymphocytes (1×10^6) were washed once in cold PBS and resuspended in 100 μL of cold PBS. Cells were either left untreated or treated with 2 μL of an antibody cocktail consisting of phycoerythryn-Cy5 (PC5)-coupled anti-CD3, phycoerythryn (RD1)-coupled anti-CD4, and fluorescein isothiocyanate (FITC)-coupled anti-CD8 (Beckman Coulter, Fullerton, CA) and incubated for 30 min on ice. Cells were then washed with PBS and fixed with 1% PFA before flow cytometry analysis (EPICS XL, Beckman Coulter).

Anti-Phosphotyrosine Western Blot. Stimulated cells were lysed in 2× loading buffer [125 μM Tris (pH 6.4), 10% β-mercaptoethanol, 8% SDS, 17.5% glycerol, 5 mM Na_3VO_4, 250 μg/mL aprotinin, 250 μg/mL leupeptin, and 0.0025% bromophenol blue], and a sample aliquot was loaded on a 7.5 to 20% gradient SDS−polyacrylamide gel. Electrophoresis was performed overnight at 5 mA per gel, and the samples were electrotransferred for 3 h at 500 mA on a PVDF membrane. The membrane's unoccupied binding sites were blocked for 1 h at 37 °C using a 1% gelatin/Tris-buffered saline/0.5% Tween-20 (TBST) solution. The membrane was then immunoblotted for 1 h at 37 °C with the mouse 4G10 antibody raised against phosphotyrosine residues at a 1:3000 concentration in a 1% gelatin/TBST solution and rinsed four times with the TBST solution. Tyrosine-phosphorylated proteins were revealed by incubating the membrane for 1 h at room temperature with a 1:20000 solution of HRP-coupled goat anti-mouse antibody (Amersham Biosciences, Piscataway, NJ) in TBST, washing four times for 10 min with TBST solution, and using ECL plus

substrate (Amersham Biosciences) as per the manufacturer's instructions.

RESULTS

NF-κB Activation by bpV Compounds Requires CD45 and p36^{LAT}. Following antigenic stimulation, activation of the *src* and *syk* family kinases leads to tyrosine phosphorylation of multiple substrates. To be fully activated, the *src* family kinase p56^{lck} requires an open conformation provided by dephosphorylation of its tyrosine 505 residue by the protein tyrosine phosphatase CD45 (*32*). CD45 deficiency in T cells causes antigenic stimulation defects at the level of CD3ζ phosphorylation. CD45 thus plays a critical role in TCR signaling by constantly maintaining an active pool of p56^{lck} that is able to respond to TCR ligation. Upon CD3ζ phosphorylation, the *syk* family kinase ZAP-70 is recruited to the TCR−CD3 complex and activated (*7*). One important substrate of ZAP-70 is p36^{LAT}, an integral membrane molecular adapter containing multiple tyrosine residues that can act as potential SH2-binding sites when phosphorylated (*10*, *31*). This molecule has been demonstrated to be critical for calcium release and activation of PKC-, PI3K-, and Ras-dependent signal transduction pathways following TCR engagement (*9*, *10*). Since both CD45 and p36^{LAT} are critical for TCR-induced signal transduction, we thus assessed the role of these signal transducers in bpV-induced NF-κB activation. To do so, we first performed EMSA experiments to study NF-κB nuclear translocation following bpV[pic] treatment in the CD45-negative J45.01 cells (*27*) and in the p36^{LAT}-negative JCAM.2 cells (*9*, *26*). Both cell lines show a drastic reduction in the level of NF-κB nuclear translocation following treatment with bpV[pic] compared with the parental Jurkat cells (Figure 1A,B). CD45 was previously described as being essential for NF-κB induction by the protein tyrosine phosphatase inhibitor pervanadate (*19*), and our results suggest a similar implication of this protein tyrosine phosphatase in bpV-induced NF-κB activation. To convincingly implicate the p36^{LAT} molecular adapter, we performed reconstitution experiments using a p36^{LAT} expression vector in the JCAM.2 cell line. Transfection of increasing amounts of the p36^{LAT} expression vector reconstituted the PMA/PHA- and bpV-mediated NF-κB transcriptional activation, while that of PMA alone remained unaffected (Figure 1C). Indeed, a 3-fold increase (from 1.9 to 5.2) in NF-κB-driven luciferase activity was observed in p36^{LAT}-reconstituted cells following bpV[pic] treatment as compared to a 2-fold enhancement in reporter gene activity following PMA/PHA stimulation (compare 16.4 and 33.6). Altogether, these experiments indicate that CD45 and p36^{LAT} are both critical effectors of the bpV-mediated NF-κB signaling pathway.

Involvement of both Calcium-Sensitive and -Insensitive PKC Isoforms in bpV-Induced NF-κB Activation. It was a logical choice then to focus our attention on p36^{LAT}-dependent signaling events. One of these is the recruitment and activation of PLCγ, which leads to hydrolysis of PIP_2 to DAG and IP_3. Generation of DAG allows PKC activation through binding of its regulatory domain and subsequent conformational change. Three different types of PKC isoforms have thus far been described: calcium- and DAG-sensitive conventional isotypes (cPKC, i.e., PKCα, PKCβ, and PKCγ), calcium-insensitive and DAG-sensitive novel isotypes (nPKC, i.e., PKCδ, PKCε, PKCη, and PKCθ), and calcium- and DAG-insensitive atypical isotypes (aPKC, i.e., PKCτ and PKCζ) (*34*, *35*). Since conventional and novel isoforms are the only ones which respond to DAG, these are the most likely to be activated following antigenic stimulation. Using PKC inhibitors targeting either the conventional or the novel PKC subtypes, we investigated

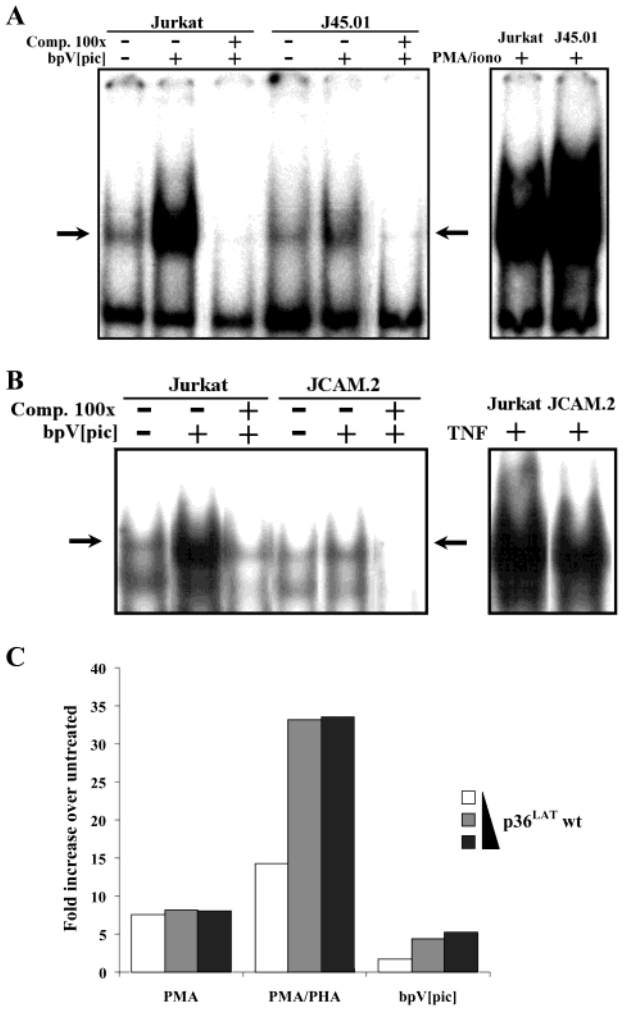

FIGURE 1: bpV-mediated NF-κB activation involves CD45 and p36^{LAT}. (A) Jurkat or CD45-deficient J45.01 cells were either left untreated or stimulated with bpV[pic] (10 μM) or PMA and ionomycin (20 ng/mL and 1 μM, respectively) for 1 h at 37 °C before nuclear extraction as described in Experimental Procedures. EMSA experiments were then performed, and translocation of NF-κB was evaluated. Cold double-stranded NF-κB oligonucleotide was used at a 100× concentration as a specific competitor. (B) Parental Jurkat or LAT-deficient JCAM.2 cells were either left untreated or stimulated with bpV[pic] (10 μM) or TNFα (20 ng/mL) for 60 min at 37 °C, and nuclear extracts were prepared as described in Experimental Procedures. EMSA experiments were then performed, and translocation of NF-κB was evaluated. Cold double-stranded NF-κB oligonucleotide was used at a 100× concentration as a specific competitor. (C) LAT-deficient JCAM.2 cells were electroporated with 5 μg of pNF-κB-LUC construct and 0 (white), 5 (gray), or 10 μg (black) of pCDNA3.1 LAT wild-type construct. The total DNA concentration was kept constant at 15 μg using the pCDNA3.1 empty vector. After 24 h, cells were stimulated with either PMA (20 ng/mL), a combination of PMA and PHA (20 ng/mL and 3 μg/mL, respectively), or bpV[pic] (10 μM) for 6 h at 37 °C. Luciferase activity was then assayed as described in Experimental Procedures. Results are represented as the fold increase of the level of activation over untreated cells and are representative of two independent experiments.

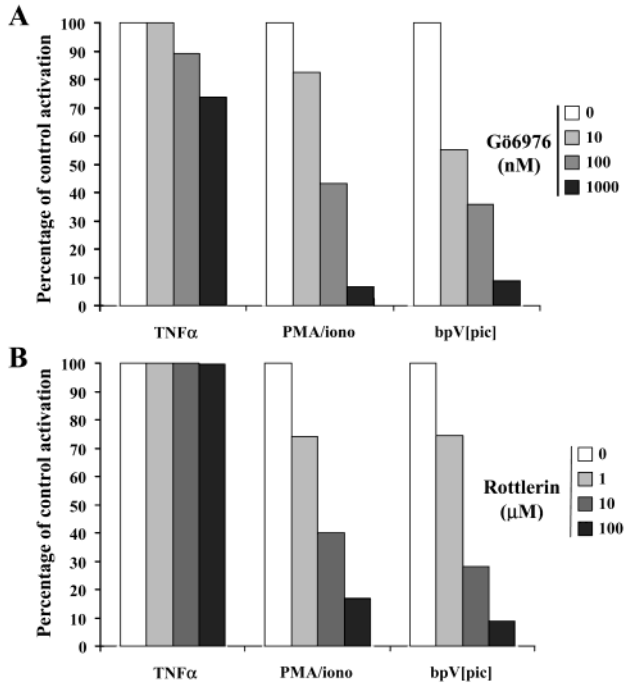

FIGURE 2: Implication of calcium-sensitive and -insensitive PKC isoforms in NF-κB activation induced by bpV compounds. (A) Jurkat cells were either left untreated or pretreated for 1 h at 37 °C with the calcium-sensitive PKC inhibitor Gö6976 (10, 100, or 1000 nM). Following this incubation, cells were stimulated with either TNF-α (20 ng/mL), a combination of PMA (20 ng/mL) and ionomycin (1 μM), or bpV[pic] (10 μM) for 6 h at 37 °C. Luciferase activity was then assayed as described in Experimental Procedures. Results are representative of three independent experiments. (B) Jurkat cells were either left untreated or pretreated for 1 h at 37 °C with the calcium-insensitive PKC inhibitor Rottlerin (1, 10, or 100 μM). Following this incubation, cells were stimulated with either TNF-α (20 ng/mL), a combination of PMA (20 ng/mL) and ionomycin (1 μM), or bpV[pic] (10 μM) for 6 h at 37 °C. Luciferase activity was then assayed as described in Experimental Procedures. Results are representative of three independent experiments.

the role of this family of enzyme in NF-κB activation induced by bpV compounds. The JκB cell line, which is a Jurkat-derived cell line stably expressing the firefly luciferase gene under the control of five consensus binding sites for NF-κB, was pretreated either with the cPKCα/β inhibitor Gö6976 (Figure 2A) or with the nPKCδ/θ inhibitor Rottlerin (Figure 2B) prior to stimulation with a combination of PMA and ionomycin as a positive control, TNFα as a negative control, and bpV[pic]. Results show that bpV-mediated NF-κB activation is clearly dependent on both PKC isotypes much like the positive control PMA and ionomycin. As previously reported, TNFα-induced NF-κB activation is independent of either PKC isotype and again demonstrates the exquisite specificity of signaling pathways between bpV compounds and TNFα.

IKKs, NIK, and TPL-2/COT Are Involved in NF-κB Activation by bpV Compounds. Previous studies indicate that degradation of IκB by the 26S proteasome is a prerequisite for nuclear translocation of NF-κB (*32*−*34*). The ubiquitin moiety which is recognized by the proteasome is added to two adjacent lysines at the N-terminus of IκBα following phosphorylation of two specific serine residues (*2*, *3*). Identification of the specific kinase phosphorylating IκBs has been a major area of research in the past years, and many candidates were proposed. Two kinases, termed IKKα (IκB

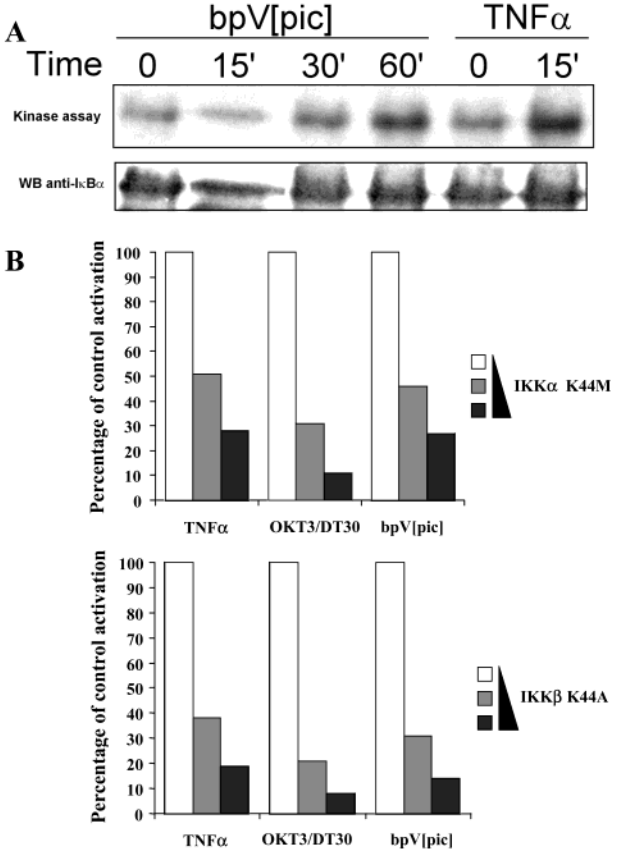

FIGURE 3: NF-κB activation by bpV compounds requires IKK activity. (A) Jurkat cells were stimulated with bpV[pic] (10 μM) for 0, 15, 30, or 60 min or with TNFα (20 ng/mL) for 0 or 15 min at 37 °C. An IκBα-specific radioactive kinase assay was performed followed by SDS−PAGE and membrane electrotransfer as described in Experimental Procedures. Results are representative of two independent experiments. (B) Jurkat cells were electroporated with 5 μg of pNF-κB-LUC construct and 0 (white), 5 (gray), or 20 μg (black) of expression vectors encoding dominant-negative versions of IKKα (pEV3T T7 IKKα K44M) or IKKβ (pCDNA3.1 IKKβ K44A). The total DNA concentration was kept constant at 25 μg using respective empty vectors. Following a 24 h incubation period, cells were stimulated with TNFα (20 ng/mL), OKT3-bearing DT30 cells (2 μg/mL, 1:10 ratio), or bpV[pic] (10 μM) for 6 h at 37 °C. Luciferase activity was assessed as described in Experimental Procedures. Results are represented as a percentage of activation of cells transfected with enzymatically inactive constructs compared with activation of cells transfected with control DNA only. Results are representative of two independent experiments.

kinase alpha) and IKKβ (IκB kinase beta), were subsequently discovered and shown by multiple independent studies to be able to interact with and specifically phosphorylate IκBα at serines 32 and 36 (*35*−*37*). An increase in the level of IκBα phosphorylation is thus indicative of increased IKK activity and NF-κB activation. To evaluate a possible activation of IKKs by bpV compounds, an *in vitro* radioactive kinase assay using full-length IκBα as a substrate was performed on immunoprecipitates of endogenous IKKs using an IKKα/β cross-reactive antibody following stimulation of Jurkat E6.1 cells with bpV[pic]. Autoradiography of the PVDF membrane following SDS−PAGE and membrane electrotransfer showed a gradual increase in IKK activity after bpV[pic] treatment (Figure 3A). TNFα stimulation induced a strong IκBα phosphorylation after 15 min, while bpV[pic] stimulation showed a delay in IKK activation and induced an IκBα phosphorylation comparable to that of

TNFα but only after stimulation for 60 min. Using another experimental strategy, cotransfection of Jurkat cells with a NF-κB-dependent reporter gene vector and increasing amounts of kinase inactive mutants of IKKα and IKKβ resulted in a dose-dependent decrease in the level of TNFα-, TCR/CD28-, and bpV-mediated activation of NF-κB (Figure 3B). These results imply that these kinases are involved in the induction of NF-κB by bpV treatment.

Upstream kinases capable of activating the IKKs include NIK (NF-κB-inducing kinase) (*36*), TPL-2/COT (*28*), and several MEKK- and MEKKK-related kinases (*38*−*40*). While NIK was shown to be necessary for both TNFα- and TCR/CD28-induced NF-κB activation, TPL-2/COT was demonstrated to be more specific for the TCR/CD28 signaling pathway (*28*). More recently, another IKK complex, different from the IKKα and IKKβ heterodimer or the IKKβ homodimer, was discovered and shown to be able to specifically phosphorylate IκBα following activation by PMA treatment or TCR/CD28 costimulation but not by TNFα stimulation (*29*). Characterization of this complex led to the discovery of IKKε (IκB kinase epsilon), capable of specifically phosphorylating serine 32 of IκBα. NIK, TPL-2/Cot, and IKKε were thus tested for their possible involvement in bpV-mediated NF-κB activation. Cotransfection of catalytically inactive mutants of NIK, TPL-2/Cot, and IKKε with a NF-κB-driven luciferase expression vector revealed an interesting dichotomy between NIK and the other kinases that were tested. While a dominant interfering NIK effectively decreased the level of NF-κB activation by all activators that were tested, catalytically inactive mutants of TPL-2/Cot and IKKε were found to more potently abrogate NF-κB activation induced by bpV[pic] and TCR/CD28 stimulation than by TNFα (Figure 4). These findings are in line with previous reports (*28*, *29*) and suggest a similarity between bpV- and TCR/CD28-induced NF-κB activation pathways.

The Kinetics of bpV-Induced NF-κB Activation Are Comparable to Those of Costimulation through both TCR and CD28. As we have previously described (*24*), NF-κB activation occurs more slowly via bpV than via TNFα. Because of the aforementioned similarity between bpV- and TCR/CD28-mediated NF-κB signaling pathways, we next carried out comparative analyses of the kinetics of NF-κB activation by these agents.

The kinetics of NF-κB-mediated transcriptional activation following TCR/CD28, TNFα, and bpV[pic] stimulation were evaluated using the Jκ B cell line. Jκ B cells were stimulated for various times with OKT3-bearing P815 cells (B7.1-negative), OKT3-bearing DT30 cells (B7.1-positive), TNFα, or bpV[pic]. Maximal NF-κB-dependent luciferase activity was achieved 4−6 h following TNFα stimulation, while maximal TCR/CD28- and bpV[pic]-induced NF-κB-mediated luciferase activity occurred 10 and 12 h, respectively, following treatment (Figure 5). As expected, OKT3-bearing P815 cells, which do not express the B7.1 costimulatory molecule, acted as a weak inducer of NF-κB.

To corroborate data from transcriptional assays, we performed EMSA analyses of Jurkat nuclear extracts using a probe specific for NF-κB binding. We therefore evaluated the kinetics of NF-κB translocation to the nucleus at various time points following treatment with TNFα, OKT3/P815, OKT3/DT30, or bpV[pic]. EMSA results confirmed our findings from transcriptional assays in that comparable kinetics of NF-κB induction were seen upon TCR/CD28 coengagement and bpV treatment (Figure 6). TNFα-induced NF-κB nuclear translocation was rapid as it occurred as early as 15 min following stimulation, and the extent of translocation decreased slowly after 1 h. In contrast, maximal nuclear translocation of NF-κB was seen at much later time points, that is, 5 and 7 h following treatment with OKT3/DT30 and bpV[pic], respectively. Stimulation of cells with OKT3-bearing P815 (B7.1-negative) cells induced a moderate and fast but very transient NF-κB nuclear translocation which returned to basal levels after stimulation for only 2 h.

All of these experiments were performed using Jurkat cells, a well-established experimental cell system. To more closely parallel physiological conditions, we next performed EMSA experiments using total PBMCs isolated from healthy blood donors and purified primary CD4+ T cell populations

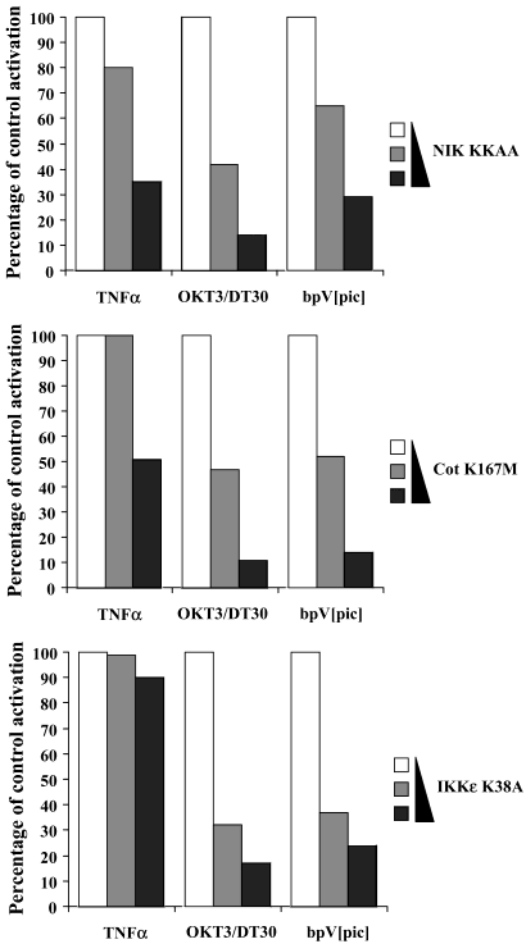

FIGURE 4: Specificity of kinases of the NF-κB signalosome complex implicated in bpV[pic]-mediated NF-κB activation. Jurkat cells were electroporated with 5 μg of pNF-κB-LUC construct and 0 (white), 5 (gray), or 20 μg (black) of expression vectors encoding dominant-negative versions of either NIK [pRKmyc NIK KK(429/430)AA], TPL-2/COT (pRK5myc TPL-2/COT K167M), or IKKε (pCDNA3.1 IKKε K38A). The total DNA concentration was kept constant at 25 μg using the respective empty vectors. Cells were then stimulated with TNFα (20 ng/mL), OKT3-bearing DT30 cells (2 μg/mL, 1:10 ratio), or bpV[pic] (10 μM) for 6 h at 37 °C. Luciferase activity was assayed as described in Experimental Procedures. Results are represented as a percentage of activation of cells transfected with enzymatically inactive constructs compared with activation of cells transfected with control DNA only. Results are representative of two independent experiments.

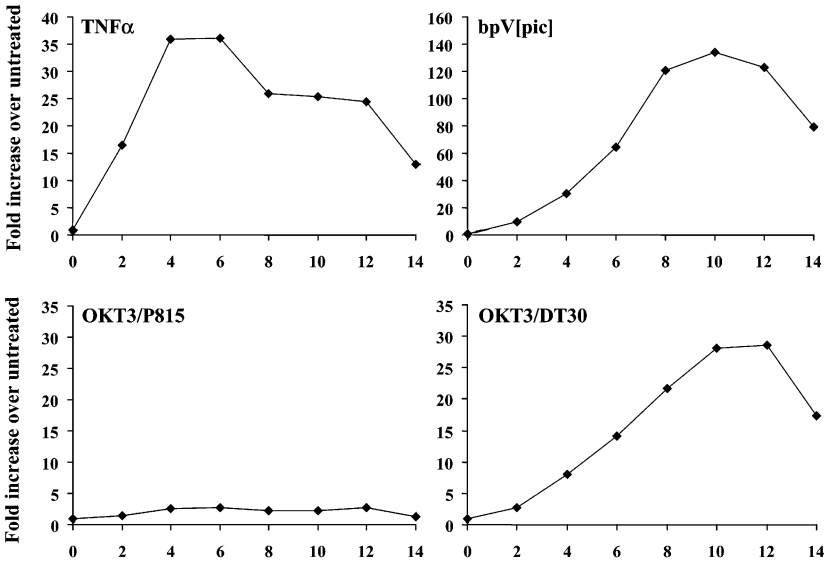

FIGURE 5: Kinetics of NF-κB transcriptional activation following TNFα, TCR, TCR/CD28, and bpV stimulation. Jurkat cells were electroporated following a standard protocol with 5 μg of pNF-κB LUC plasmid and incubated for 24 h at 37 °C before stimulation with TNFα (20 ng/mL), OKT3-bearing P815 cells (2 μg/mL, 1:10 ratio), OKT3-bearing DT30 cells (2 μg/mL, 1:10 ratio), or bpV[pic] (10 μM) for 0, 2, 4, 6, 8, 10, 12, or 14 h at 37 °C. Luciferase activity was then assayed as described in Experimental Procedures. Results are represented as the fold increase in the level of activation over untreated cells and are representative of three independent experiments.

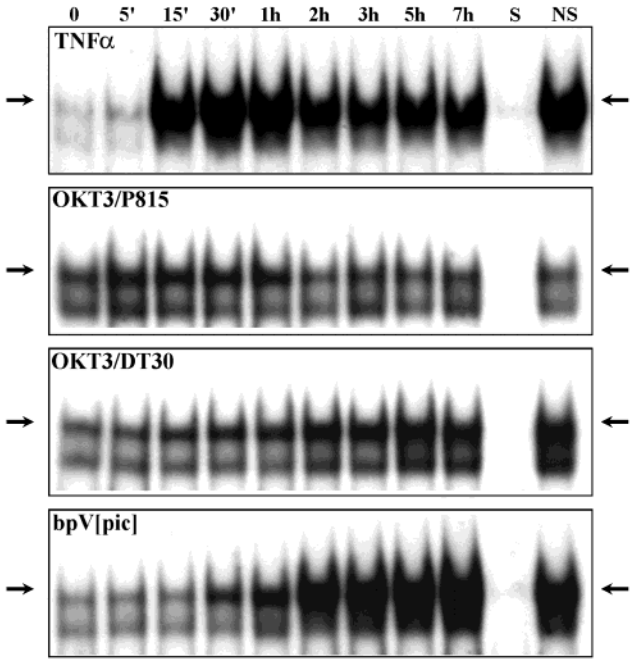

FIGURE 6: Kinetics of NF-κB nuclear translocation in Jurkat cells after treatment with TNFα, OKT3-bearing P815 cells (TCR), OKT3-bearing DT30 cells (TCR/CD28), and bpV[pic]. Jurkat cells were stimulated with TNFα (20 ng/mL), OKT3-bearing DT30 cells (2 μg/mL, 1:10 ratio), OKT3-bearing P815 cells (2 μg/mL, 1:10 ratio), or bpV[pic] (10 μM) for 0, 5, 15, or 30 min and 1, 2, 3, 5, or 7 h at 37 °C. Nuclear extracts were then prepared, and an EMSA was performed as described in Experimental Procedures. Cold double-stranded NF-κB and AP-1 oligonucleotides were used at a 100× concentration for competition assays. Specific (S) and nonspecific (NS) competitions were achieved for cells treated for 1 h with TNFα or for 5 h with OKT3/DT30, OKT3/P815, and bpV[pic]. Results are representative of two independent experiments.

originating from these PBMCs. Purification of CD4+ T lymphocytes was performed by negative selection with the use of a StemSep magnetic beads and columns system (see Experimental Procedures). This purification procedure routinely yielded a 95% pure CD3+/CD4+ T cell population as monitored by FACS analysis with no detectable CD8+ cells (data not shown). Total PBMCs and purified CD4+ primary T cells were deprived of IL-2 1 day before treatment with TNFα, OKT3-bearing DT30 cells, or bpV[pic]. Results obtained from the total PBMC population showed a high degree of similarity between TNF- and TCR/CD28-induced NF-κB activation kinetics compared to those obtained using Jurkat cells (Figure 7). Conversely, bpV[pic]-induced NF-κB activation displayed slightly different kinetics in PBMCs and Jurkat cells. Between the 1 and 2 h time points, the extent of localization of NF-κB to the nucleus of PBMC increased sharply, and a peak was reached between 2 and 5 h. This surge of NF-κB translocation was also seen in OKT3/DT30-stimulated extracts but at a lower level between the 1 and 2 h time points for PBMC nuclear extracts.

EMSA experiments using primary CD4+ T cells showed similar kinetics of NF-κB nuclear translocation compared with those for total PBMCs for each stimulus that was tested. TNFα stimulation induces a fast and sharp induction of NF-κB during the first hour, and the level of stimulation slowly decreases from then on (Figure 8). OKT3/DT30 and bpV[pic] stimulations cause a slow and delayed type of response in which NF-κB begins to appear in the nucleus 1−2 h poststimulation and peaked at 3−5 h but remained high at the 7 h time point.

Bisperoxovanadium Compound Treatment and TCR/CD28 Engagement Initiate Distinct Patterns and Kinetics of Protein Tyrosine Phosphorylation. Even though NF-κB induction effectively seems to proceed in an analogous, but not identical, mode with bpV or TCR/CD28 stimulation, we decided to compare tyrosine phosphorylation events mediated by these two stimulating agents. Anti-phosphotyrosine Western blot experiments revealed an interesting distinction in both the intensity and kinetics of protein tyrosine phosphorylation induced by bpV compounds compared with a TCR/CD28 costimulation. Serum-starved Jurkat cells were exposed to bpV[pic] or OKT3-bearing DT30 cells for 1, 2,

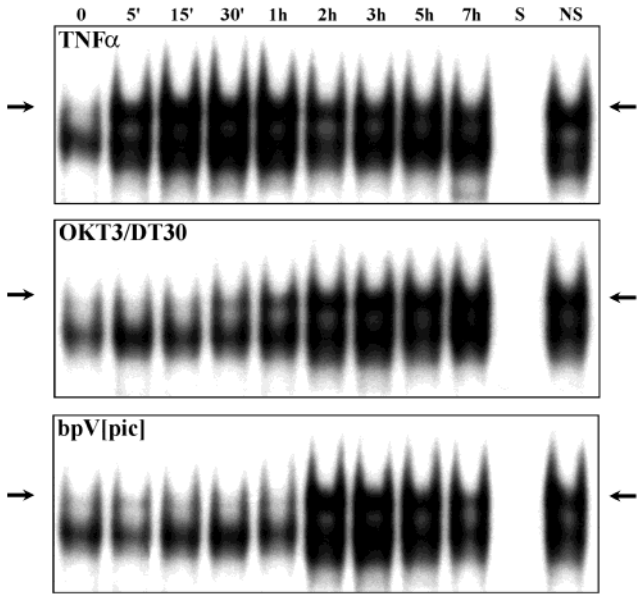

FIGURE 7: Kinetics of NF-κB nuclear translocation in PBMCs after treatment with TNFα, OKT3-bearing DT30 cells (TCR/CD28), or bpV[pic]. One day IL-2-starved PBMCs were stimulated with TNFα (20 ng/mL), OKT3-bearing DT30 cells (2 μg/mL, 1:10 ratio), or bpV[pic] (10 μM) for 0, 5, 15, or 30 min and 1, 2, 3, 5, or 7 h at 37 °C. Nuclear extracts were then prepared, and an EMSA was performed as described in Experimental Procedures. Cold double-stranded NF-κB and AP-1 oligonucleotides were used at a 100× concentration for competion assays. Specific (S) and nonspecific (NS) competitions were achieved for cells treated for 1 h with TNFα or for 5 h with OKT3/DT30 and bpV[pic]. Results are representative of two independent experiments.

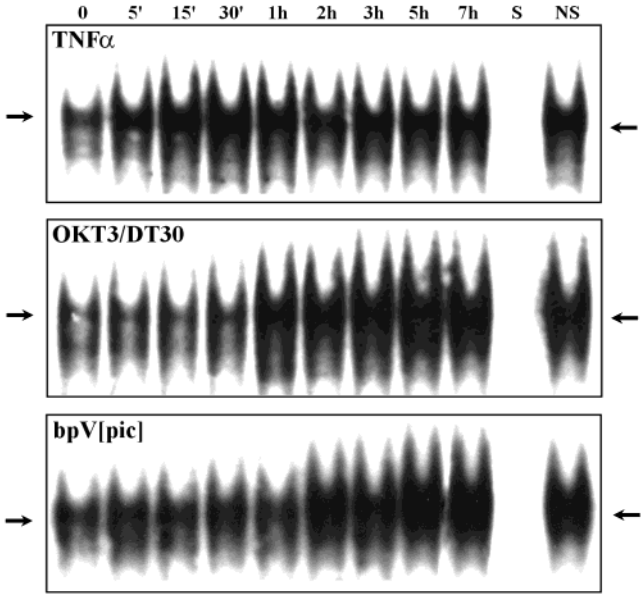

FIGURE 8: Kinetics of NF-κB nuclear translocation in primary CD4+ T lymphocytes after treatment with TNFα, OKT3-bearing DT30 cells (TCR/CD28), and bpV[pic]. One day IL-2-starved primary CD4+ T lymphocytes were stimulated with TNFα (20 ng/mL), OKT3-bearing DT30 cells (2 μg/mL, 1:10 ratio), or bpV[pic] (10 μM) for 0, 5, 15, or 30 min and 1, 2, 3, 5, or 7 h at 37 °C. Nuclear extracts were then prepared, and an EMSA was performed as described in Experimental Procedures. Cold double-stranded NF-κB and AP-1 oligonucleotides were used at a 100× concentration for competition assays. Specific (S) and nonspecific (NS) competitions were achieved for cells treated for 1 h with TNFα or for 5 h with OKT3/DT30 and bpV[pic]. Results are representative of two independent experiments.

5, 10, 20, or 30 min, lysed, and subjected to SDS−polyacrylamide gel electrophoresis (i.e., gradient from 7.5 to 20%). The gradient gel was electrotransferred to a PVDF membrane that was finally blotted with an anti-phosphotyrosine antibody (clone 4G10). Significant differences at the level of tyrosine phosphorylation can be seen between the two treatment groups (Figure 9). First, protein tyrosine phosphorylation induced by bpV[pic] appears more slowly and reaches a peak 20 min after addition of bpV, whereas TCR/CD28-induced protein tyrosine phosphorylation appears much faster and also on a more restricted set of proteins. Second, the intensity and number of detected tyrosine-phosphorylated proteins are greater in cells stimulated with bpV[pic] than in those stimulated with OKT3-bearing DT30 cells. Thus, abrogation of PTP activity by bpV compounds initiates a slow, sustained, and robust phosphorylation of tyrosine residues different from the rapid, transient, and discreet tyrosine phosphorylation induced by TCR/CD28 coengagement.

DISCUSSION

Control of signal transduction by PTP has emerged as a paradigm for cellular deactivation or repression of activation. Recent discoveries in this field seem to suggest that for any given PTK implicated in signal generation, a counteracting PTP capable of inhibiting or repressing the signal initiated by the PTK may exist. Regulation of PTP expression, activity, and localization is thus as important to understand as it is for PTK. Keeping in mind that cellular hyper- or hyporesponsiveness is a function of both PTK and PTP activities, we find it rather interesting that upon treatment of cells with a potent and specific PTP inhibitor such as bpV[pic], the signaling cascade that leads to NF-κB retains most of the effectors needed for normal activation via a TCR/CD28 costimulation.

In this study, we first evaluated whether the CD45 protein tyrosine phosphatase played a role in bpV-mediated NF-κB activation. EMSA experiments comparing the CD45-positive Jurkat and the CD45-negative J45.01 NF-κB nuclear translocation following bpV treatment (Figure 1A) ascribe a role to CD45 similar to the one suggested by Imbert et al. regarding pervanadate-induced NF-κB activation (*19*). CD45 deficiency drastically reduces the level of bpV-induced NF-κB activation probably in a fashion similar to TCR-induced NF-κB activation. Indeed, since $p56^{lck}$ activation was reported to be crucial to NF-κB induction by bpV compounds and CD45 is no longer present to keep an active pool of $p56^{lck}$ in the J45.01 cell line, it is only logical that NF-κB activation by bpV compounds is abrogated in such circumstances. Still, it is interesting to question why inhibition of CD45 by bpV compounds does not lead to an outcome similar to CD45 deficiency. In this case, much like an antigenic stimulation, it seems that CD45 plays both a positive and a negative role. By keeping an active pool of dephosphorylated $p56^{lck}$, CD45 keeps the cell responsive to bpV compounds that will induce phosphorylation of $p56^{lck}$ on tyrosine 394 of its activation loop. Even if bpV compounds inhibit CD45, the active pool of $p56^{lck}$ remains in a dephosphorylated state for a sufficiently long time for activation to occur. From this point on, tyrosine

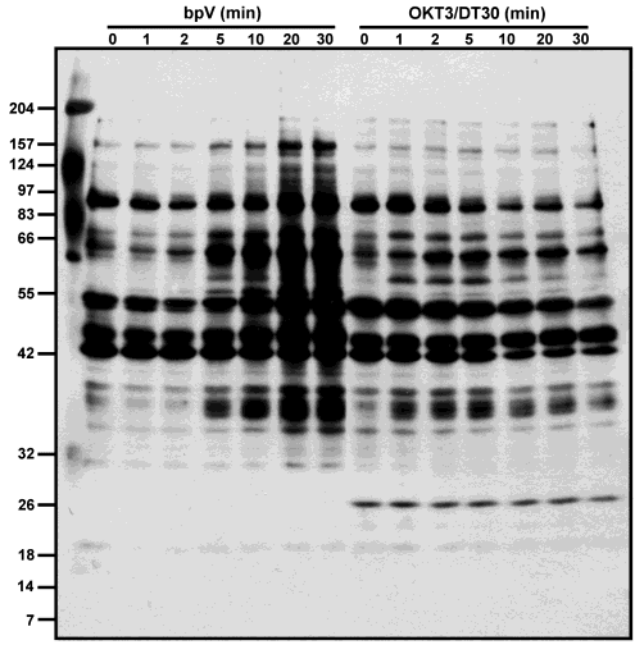

FIGURE 9: Kinetic studies assessing protein tyrosine phosphorylation events upon bpV treatment and TCR/CD28 costimulation. Jurkat cells (1×10^6 per sample) were stimulated with either 10 μM bpV[pic] or OKT3-bearing DT30 cells as described in Experimental Procedures for 0, 1, 2, 5, 10, 20, or 30 min at 37 °C. Cells were then lysed in 2× loading buffer; a sample aliquot corresponding to 4×10^5 cells was loaded on a 7.5 to 20% gradient SDS−polyacrylamide gel, and an anti-phosphotyrosine Western blot was performed as described in Experimental Procedures.

kinase activity in the cell is almost completely unhindered and signal generation can proceed. The presence of CD45 is thus needed for bpV-mediated NF-κB induction even if CD45 is itself a target of these compounds.

In an earlier report, ZAP-70 and SLP-76 were shown to be necessary for optimal NF-κB activation by bpV molecules (*24*). This work led us to postulate that the molecular adapter and ZAP-70 substrate $p36^{LAT}$ could be an important mediator of bpV-generated signaling events. EMSA experiments show similar NF-κB nuclear translocation induced by TNFα in Jurkat and JCAM.2 cell lines, while bpV[pic] induced a very weak NF-κB nuclear translocation in $p36^{LAT}$-deficient JCAM.2 cells compared with the translocation of the parental cell line (Figure 1B). Transient reconstitution of $p36^{LAT}$ in LAT-deficient JCAM.2 cells further demonstrates a role for this molecular adapter in bpV-induced NF-κB activation as a 3-fold increase in NF-κB-driven luciferase activity ensues while PMA-induced NF-κB activation remains unaffected (Figure 1C). These results provide strong evidence that $p36^{LAT}$, like CD45 and $p56^{lck}$, is a very important mediator of NF-κB signaling induced by bpV molecules. Although ZAP-70 and SLP-76 are not absolutely essential, CD45, $p56^{lck}$, and $p36^{LAT}$ are definitely required for bpV-mediated activation of NF-κB. Since the TCR−CD3 complex was already shown to be unnecessary for bpV-induced NF-κB induction (*24*), phosphorylation of a membrane-anchored and lipid raft-targeted adapter containing multiple SH2-binding sites such as $p36^{LAT}$ following PTP inhibition by bpV molecules could thus lead to the formation of a signaling complex requiring $p56^{lck}$ activity for signal generation. This working hypothesis is schematically described in Figure 10 and represents our current model regarding activation of NF-κB by bpV compounds in CD4 T cells. Although some pieces are still missing and others are clearly inspired from previous reports of TCR/CD28 signal transduction, this working hypothesis is currently dictating our future research avenues.

It has been known for many years now that PKC activation via phorbol esters or the classical TCR/CD28 pathway leads to NF-κB activation. It has been only recently, however, that the link between PKC and NF-κB in the antigenic stimulation pathway was uncovered with the finding that PKCθ was essential for NF-κB induction following TCR and CD28 ligation. From then on, PKCθ became a major target of research since its implication in the antigenic stimulation pathway seems to be quite specific and its inhibition could thus lead to the discovery of potent and specific drugs for allograft rejection or other autoimmune disease-implicating T cells. We used two pharmacological inhibitors specific for either calcium-sensitive cPKC or calcium-insensitive nPKC to evaluate the role of PKCα/β and PKCδ/θ in bpV-mediated NF-κB activation. Inhibition of NF-κB transcriptional activation by the PKCα/β inhibitor Gö6976 and the PKCδ/θ inhibitor Rottlerin was observed with PMA and ionomycin as well as bpV[pic] treatment in a dose-dependent manner, while TNFα stimulation remained unaffected. These results imply a serial pathway where both calcium-sensitive and -insensitive PKC play a role in bpV-induced NF-κB activation. Thus, while PKCθ is important for NF-κB induction by bpV compounds much like the TCR/CD28 pathway, it also seems that another PKC, either PKCα or PKCβ, is critical for bpV-mediated signal transduction to NF-κB. Since the link between PKCθ and IKKβ has been established as a direct one and PKCθ can induce NF-κB activation by itself (*41*), it is reasonable to assume that the calcium-sensitive PKC implicated in the bpV-induced pathway is upstream of PKCθ. Further study of this PKC relationship is indicated as it probably could also be applied to the TCR/CD28 pathway.

The importance of NF-κB control in a normal immune system is underscored by the presence of multiple specific and highly regulated kinases implicated in its release from IκBs but also in its transcriptional activation and interaction with other transcription factors and the transcriptional machinery. We thus monitored whether bpV[pic] treatment resulted in activation of IκB kinases by performing an IκBα-specific *in vitro* kinase assay. This experiment provides for the first time direct evidence of IκB kinase activation by protein tyrosine phosphatase inhibitors. Moreover, results from this series of investigations clearly show differences between bpV[pic] and TNFα kinetics of IκB kinase activation as TNFα induces a strong IκBα phosphorylation in 15 min while bpV[pic] requires at least 60 min to produce a comparable signal (Figure 3A). Further investigation using dominant interfering enzymes led us to identify five important kinases implicated in bpV-mediated NF-κB activation. These kinases have been previously described for their importance in NF-κB activation by TCR/CD28 costimulation (*28*, *29*). Our studies on the implication of such kinases in bpV-mediated NF-κB activation revealed that IKKα, IKKβ, and NIK are implicated in NF-κB-mediated transcriptional activation by all activators that were tested (i.e., TNFα, TCR/CD28, and bpV[pic]) (Figures 3B and 4), while TPL-2/COT and IKKϵ are especially implicated in bpV- and TCR/CD28-derived signals (Figure 4). These data when coupled with

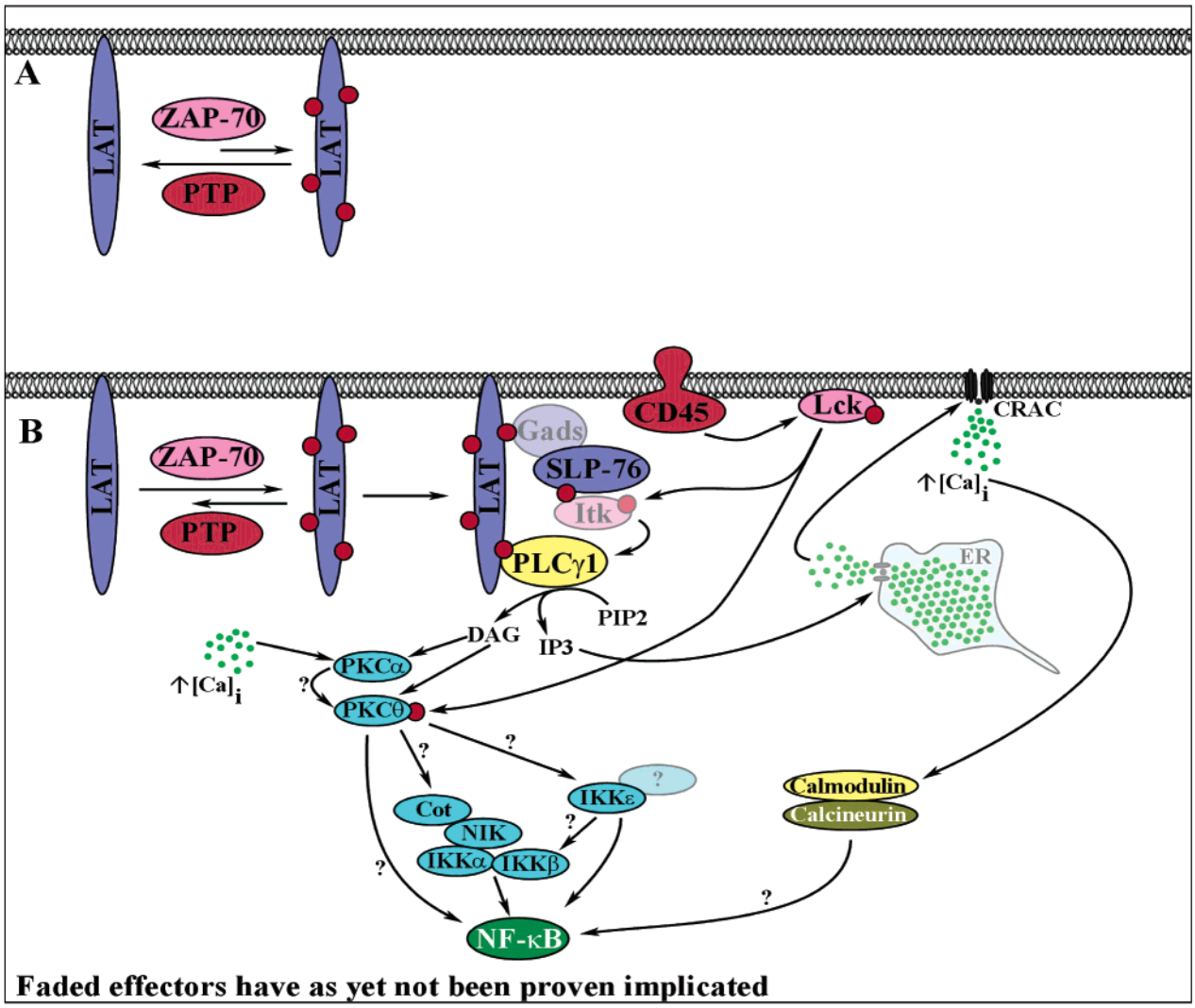

FIGURE 10: Working hypothesis for NF-κB activation in $CD4^+$ T lymphocytes by bpV compounds. (A) Untreated or resting T cells display a hypophosphorylated $p36^{LAT}$ due to high constitutive PTP activity and low PTK activity. (B) Upon bpV treatment, PTP activity is abrogated and PTK activity is sufficient to lead to $p36^{LAT}$ phosphorylation and the recruitment of SLP-76 possibly via Grb2-like molecular adapters. SLP-76 could localize *Tec* family PTK such as Itk to the membrane, activation of which is dependent on phosphorylation of its activation loop by $p56^{lck}$. Upon activation, Itk could phosphorylate $p36^{LAT}$-associated PLCγ and lead to catalysis of PIP_2 to IP_3 and DAG, two critical second messengers required for calcium mobilization and PKC activation, respectively. After the intracellular calcium stores had been emptied, capacitative entry of calcium induces a high and sustained intracellular concentration of calcium ions and activates calcium-sensitive enzymes such as PKCα and the serine/threonine phosphatase calcineurin which have an undeniable (although still enigmatic) effect on NF-κB activation. Activation of PKCθ through tyrosine phosphorylation by $p56^{lck}$ and binding of DAG could induce IKK complex activation directly or via TPL-2/Cot and NIK and lead to phosphorylation and degradation of IκB and subsequent NF-κB nuclear translocation and transcriptional activation.

previous reports (*28*, *29*) suggest strong similarities between TCR/CD28- and bpV-activated signal transduction pathways, while a distinct signaling pathway is engaged by TNFα. It is interesting to note that inhibition of NF-κB activation by each dominant negative kinase, and especially for IKKα and NIK, was always weaker for bpV[pic] than for TCR/CD28 costimulation. This could imply that a stronger signal is generated by bpV compounds which would be more difficult to inhibit or alternatively that a bypass mechanism could exist that involves as yet unknown IKKs or other mechanisms of NF-κB activation such as tyrosine phosphorylation events (*18*).

Kinetic studies of NF-κB-dependent reporter gene transcriptional assays (Figure 5) and NF-κB nuclear localization by EMSA experiments (Figures 6−8) revealed interesting features of the signaling cascades initiated by the stimulating agents that were tested (i.e., bpV, TCR/CD28, and TNFα). While TNFα-mediated induction of NF-κB was rapid, TCR/CD28 costimulation and bpV[pic] treatment induced a much slower response. TCR stimulation alone induced a weak NF-κB-mediated transcription of the luciferase reporter gene and a strong and fast but highly transient NF-κB nuclear localization which clearly indicates a crucial role for the CD28 pathway in strong and sustained NF-κB-dependent gene activation. To the best of our knowledge, this kinetic study is the first one that has used such highly physiologically relevant methods to achieve TCR/CD28 costimulation (i.e., OKT3-bearing B7.1-positive DT30 cells). Moreover, the similarity between the bpV[pic]- and TCR/CD28-induced kinetics of NF-κB activation and their distinction from TNFα kinetics further accentuate the shared signaling pathways between bpV compounds and TCR/CD28 engagement.

Kinetics of bpV-induced NF-κB nuclear translocation in primary cells showed slight differences compared with those of Jurkat T cells, peaking 1 or 2 h earlier. This could be due to variations in the overall pattern of PTP expression between primary and Jurkat T cells or to the existence of better mechanisms of signal termination in primary T lymphocytes. A slight delay (i.e., 15 min to 1 h) in NF-κB nuclear translocation following treatment with either TCR/CD28 or bpV could also be observed between primary T cells and Jurkat cells. This phenomenon could be linked with an already described hyperresponsiveness of Jurkat cells to TCR-mediated signals due to a PTEN deficiency (*42*). This deficiency could enhance the kinetics of signal generation since PI3K activity and PIP_3 accumulation would not be required prior to signaling complex formation and initiation of the signaling cascade. Confirming that differences in NF-κB activation kinetics are specific for the TCR pathway, we found no significant variation in NF-κB nuclear localization kinetics for TNFα stimulation between primary T lymphocytes and Jurkat cells. Notwithstanding minor differences in NF-κB activation kinetics in primary cells and Jurkat cells, bpV compounds thus effectively resemble TCR/CD28-induced signaling events in their ability to induce a slow but sustained increase in the level of NF-κB nuclear localization.

Induction of NF-κB activation by either bpV compounds or TCR/CD28 costimulation occurs through a tyrosine phosphorylation-dependent signaling pathway that leads to IKK complex activation and subsequent IκB degradation. Tyrosine protein phosphorylation patterns of whole cell extracts can provide an interesting insight into the most proximal events leading to NF-κB activation and how each activation pathway can achieve it. Clear differences regarding the intensity and kinetics of protein tyrosine phosphorylation were seen between Jurkat cells following stimulation with bpV[pic] and OKT3-bearing DT30 cells (Figure 9). Because the mode of action of each stimulus was entirely different, such results were somewhat expected. TCR/CD28 stimulation induces specific PTK activity on a restricted set of receptors, enzymes, and molecular adapters. On the other hand, by inhibiting PTP activity, bpV compounds progressively allow protein tyrosine phosphorylation of a large number of proteins, including those specifically associated with the TCR/CD28 complex. Such an increase in the number of tyrosine-phosphorylated proteins leads to the progressive formation of biologically relevant signaling complexes that culminate in activation of transcription factors, including NF-κB. It is interesting to note that differences observed in the kinetics of protein tyrosine phosphorylation do not necessarily translate to remarkable differences in the kinetics of NF-κB activation. This could be due to a certain threshold level of tyrosine-phosphorylated proteins that must be reached by both stimulating agents for efficient activation of NF-κB and/or to a relatively slow formation of signaling complexes leading to the NF-κB activation pathway that would minimize such differences.

In summary, by inhibiting PTP activity within a T cell, bpV compounds can induce a signaling cascade leading to NF-κB activation that is highly reminiscent of the physiological TCR/CD28 costimulation pathway. Effectors studies and time-course experiments show a high level of similarity between TCR/CD28 and bpV[pic] stimulation leading to NF-κB transcriptional activation and nuclear translocation in Jurkat cells. Moreover, nuclear localization experiments using primary human T cells suggest that the results obtained with the Jurkat model could very well be applied in a more physiological cell system.

The study of compounds that can control NF-κB and, more importantly, the understanding of their mode of action are essential for the development of better therapeutic options in the treatment of multiple autoimmune disease, pathologies, and infectious diseases, including AIDS.

ACKNOWLEDGMENT

We thank Dr. A. Weiss for the JCAM.2 cell line and the $p36^{LAT}$ expression vector. We also thank Dr. T. Maniatis for the catalytically inactive IKKε expression vector. Thanks to Dr. M. Dufour for FACS analysis and Dr. Benoit Barbeau for critical reading of the manuscript and helpful discussions.

REFERENCES

1. Baeuerle, P. A., and Baltimore, D. (1988) *Science 242*, 540−546.
2. Ghosh, S., and Baltimore, D. (1990) *Nature 344*, 678−682.
3. Mellits, K. H., Hay, R. T., and Goodbourn, S. (1993) *Nucleic Acids Res. 21*, 5059−5066.
4. Malek, S., Huxford, T., and Ghosh, G. (1998) *J. Biol. Chem. 273*, 25427−25435.
5. Barber, E. K., Dasgupta, J. D., Schlossman, S. F., Trevillyan, J. M., and Rudd, C. E. (1989) *Proc. Natl. Acad. Sci. U.S.A. 86*, 3277−3281.
6. Chan, A. C., Iwashima, M., Turck, C. W., and Weiss, A. (1992) *Cell 71*, 649−662.
7. Wange, R. L., Kong, A. N., and Samelson, L. E. (1992) *J. Biol. Chem. 267*, 11685−11688.
8. Weiss, A., Chan, A. C., Iwashima, M., Straus, D., and Irving, B. A. (1992) *Cold Spring Harbor Symp. Quant. Biol. 57*, 107−116.
9. Finco, T. S., Kadlecek, T., Zhang, W., Samelson, L. E., and Weiss, A. (1998) *Immunity 9*, 617−626.
10. Zhang, W., Sloan-Lancaster, J., Kitchen, J., Trible, R. P., and Samelson, L. E. (1998) *Cell 92*, 83−92.
11. Su, Y. W., Zhang, Y., Schweikert, J., Koretzky, G. A., Reth, M., and Wienands, J. (1999) *Eur. J. Immunol. 29*, 3702−3711.
12. Ching, K. A., Kawakami, Y., Kawakami, T., and Tsoukas, C. D. (1999) *J. Immunol. 163*, 6006−6013.
13. Lu, Y., Cuevas, B., Gibson, S., Khan, H., LaPushin, R., Imboden, J., and Mills, G. B. (1998) *J. Immunol. 161*, 5404−5412.
14. Marengere, L. E., Okkenhaug, K., Clavreul, A., Couez, D., Gibson, S., Mills, G. B., Mak, T. W., and Rottapel, R. (1997) *J. Immunol. 159*, 3220−3229.
15. Heyeck, S. D., Wilcox, H. M., Bunnell, S. C., and Berg, L. J. (1997) *J. Biol. Chem. 272*, 25401−25408.
16. Tuosto, L., Michel, F., and Acuto, O. (1996) *J. Exp. Med. 184*, 1161−1166.
17. Bubeck Wardenburg, J., Pappu, R., Bu, J. Y., Mayer, B., Chernoff, J., Straus, D., and Chan, A. C. (1998) *Immunity 9*, 607−616.
18. Imbert, V., Rupec, R. A., Livolsi, A., Pahl, H. L., Traenckner, E. B., Mueller-Dieckmann, C., Farahifar, D., Rossi, B., Auberger, P., Baeuerle, P. A., and Peyron, J. F. (1996) *Cell 86*, 787−798.
19. Imbert, V., Farahifar, D., Auberger, P., Mary, D., Rossi, B., and Peyron, J. F. (1996) *J. Inflammation 46*, 65−77.
20. Imbert, V., Peyron, J. F., Farahi Far, D., Mari, B., Auberger, P., and Rossi, B. (1994) *Biochem. J. 297*, 163−173.
21. Secrist, J. P., Burns, L. A., Karnitz, L., Koretzky, G. A., and Abraham, R. T. (1993) *J. Biol. Chem. 268*, 5886−5893.
22. Huyer, G., Liu, S., Kelly, J., Moffat, J., Payette, P., Kennedy, B., Tsaprailis, G., Gresser, M. J., and Ramachandran, C. (1997) *J. Biol. Chem. 272*, 843−851.
23. Posner, B. I., Faure, R., Burgess, J. W., Bevan, A. P., Lachance, D., Zhang-Sun, G., Fantus, I. G., Ng, J. B., Hall, D. A., Lum, B. S., et al. (1994) *J. Biol. Chem. 269*, 4596−4604.
24. Ouellet, M., Barbeau, B., and Tremblay, M. J. (1999) *J. Biol. Chem. 274*, 35029−35036.
25. Gillis, S., and Watson, J. (1980) *J. Exp. Med. 152*, 1709−1719.
26. Straus, D. B., and Weiss, A. (1992) *Cell 70*, 585−593.

27. Geleziunas, R., Ferrell, S., Lin, X., Mu, Y., Cunningham, E. T., Jr., Grant, M., Connelly, M. A., Hambor, J. E., Marcu, K. B., and Greene, W. C. (1998) *Mol. Cell. Biol. 18*, 5157−5165.
28. Lin, X., Cunningham, E. T., Jr., Mu, Y., Geleziunas, R., and Greene, W. C. (1999) *Immunity 10*, 271−280.
29. Peters, R. T., Liao, S. M., and Maniatis, T. (2000) *Mol. Cell 5*, 513−522.
30. Barbeau, B., Bernier, R., Dumais, N., Briand, G., Olivier, M., Faure, R., Posner, B. I., and Tremblay, M. (1997) *J. Biol. Chem. 272*, 12968−12977.
31. von Willebrand, M., Williams, S., Tailor, P., and Mustelin, T. (1998) *Cell Signalling 10*, 407−413.
32. Traenckner, E. B., Wilk, S., and Baeuerle, P. A. (1994) *EMBO J. 13*, 5433−5441.
33. Chen, Z., Hagler, J., Palombella, V. J., Melandri, F., Scherer, D., Ballard, D., and Maniatis, T. (1995) *Genes Dev. 9*, 1586−1597.
34. Li, C. C., Dai, R. M., and Longo, D. L. (1995) *Biochem. Biophys. Res. Commun. 215*, 292−301.
35. Mercurio, F., Zhu, H., Murray, B. W., Shevchenko, A., Bennett, B. L., Li, J., Young, D. B., Barbosa, M., Mann, M., Manning, A., and Rao, A. (1997) *Science 278*, 860−866.
36. Woronicz, J. D., Gao, X., Cao, Z., Rothe, M., and Goeddel, D. V. (1997) *Science 278*, 866−869.
37. DiDonato, J. A., Hayakawa, M., Rothwarf, D. M., Zandi, E., and Karin, M. (1997) *Nature 388*, 548−554.
38. Lee, F. S., Peters, R. T., Dang, L. C., and Maniatis, T. (1998) *Proc. Natl. Acad. Sci. U.S.A. 95*, 9319−9324.
39. Hehner, S. P., Hofmann, T. G., Ushmorov, A., Dienz, O., Wing-Lan Leung, I., Lassam, N., Scheidereit, C., Droge, W., and Schmitz, M. L. (2000) *Mol. Cell. Biol. 20*, 2556−2568.
40. Li, X., Commane, M., Nie, H., Hua, X., Chatterjee-Kishore, M., Wald, D., Haag, M., and Stark, G. R. (2000) *Proc. Natl. Acad. Sci. U.S.A. 97*, 10489−10493.
41. Lin, X., O'Mahony, A., Mu, Y., Geleziunas, R., and Greene, W. C. (2000) *Mol. Cell. Biol. 20*, 2933−2940.
42. Shan, X., Czar, M. J., Bunnell, S. C., Liu, P., Liu, Y., Schwartzberg, P. L., and Wange, R. L. (2000) *Mol. Cell. Biol. 20*, 6945−6957.

BI034013B